A study of the nonionizing component of the cosmic radiation underground



1972 J. Phys. A: Gen. Phys. 5 745

(http://iopscience.iop.org/0022-3689/5/5/016)

J. Phys. A: Gen. Phys., Vol. 5, May 1972. Printed in Great Britain

# A study of the nonionizing component of the cosmic radiation underground

J C BARTON and C M POURGOURIDES

Department of Physics, The Polytechnic of North London, London N7 8DB, UK

MS received 2 November 1971

**Abstract.** An efficient anticoincidence screen has been designed and operated in the Holborn underground laboratory at a depth of 61 hg cm$^{-2}$ below the surface. A series of experiments, using different types of counter inside this screen, were performed to study the properties of the underground nonionizing radiation at energies greater than 5 MeV. It was established that the leakage of muons through the screen was very small. The rate of neutron knock-on events was found to be 1·8 l$^{-1}$ d$^{-1}$ for protons of energy greater than 12 MeV. The rate of events due to photons of energy greater than 10 MeV was about 15 l$^{-1}$ d$^{-1}$. The origin of these photons is discussed, and it is argued that most of them are due to the bremsstrahlung of electrons knocked on by muons. No evidence is found for any anomalous behaviour of the cosmic radiation underground.

## 1. Introduction

There are two main purposes in studying the nonionizing component of cosmic radiation underground. Firstly, there is the general need to increase our knowledge of high energy cosmic rays and, in particular, to investigate the production of muons by a neutral component which has been reported by Cowan *et al* (1965 and 1969). Secondly, the nonionizing component contributes to the background counting rate of large counters in experiments such as those which have been carried out to test the validity of the hadron conservation law (Giamati and Reines 1962, Kropp and Reines 1965) and those which are at present being discussed for the detection of solar or stellar neutrinos. In these experiments it is necessary to detect a very rare type of process in the presence of a vastly greater rate due to the interaction of the background radiation. Although extreme measures have been taken to reduce this background effect, such as working deep underground and surrounding the detector with an anticoincidence counter system, very few systematic studies have been made of its precise nature.

A number of practical designs of large volume anticoincidence arrangements have been reported (see for example Stenberg and Olsson 1968, Wogman *et al* 1969, Giamati and Reines 1962, Moe *et al* 1964 and Cowan *et al* 1965) operating at various depths underground. In spite of very careful precautions, events have been observed in which particles failed to be detected by the anticoincidence screening and interacted in the principal detector. Some controversy arises about the interpretation of such events, especially in the energy region above 10 MeV where there should be no contribution from natural radioactivity. In this region there is very little experimental evidence as to whether the effects which are observed are correctly attributed to cosmic rays and, if so, which are the processes involved. This problem was appreciated by Kropp and

Reines (1965) who, considering the various sources of events in an anticoincidence counter, point out that the greatest ambiguities arise from (i) scattered low energy cosmic rays leaking into the system due to incomplete screening, and (ii) high energy gamma rays of uncertain origin.

In the present experiment, source (i) was eliminated by employing $4\pi$ anticoincidence screening. Furthermore, the apparatus was designed as an anticoincidence 'facility', which would enable various types of detector to be operated inside the screen without having to disturb its operation, so that various aspects of the nonionizing radiation could be explored. The results obtained during its two years of operation at the Holborn underground laboratory, at a depth of 61 hg cm$^{-2}$ below sea level, form the subject of the present work. Brief accounts of parts of this work have been reported at conferences in Budapest and La Paz in 1969 and 1970 respectively.

## 2. Apparatus

### 2.1. The anticoincidence screen

The main part of the screen (figure 1) was provided by an annular cylinder, closed at the lower end and open over its full diameter at the top, which was filled with a medicinal paraffin type of liquid scintillator (Barton *et al* 1962). The annulus was formed between two coaxial cylinders, made by Visijar Ltd of ordinary Perspex sheet (ICI) 6·5 mm thick, with their axes vertical. The 9 cm gap between the two cylinders was maintained by a 2 cm thick flat ring, also made of Perspex and cemented at the base of each cylinder.

The larger cylinder, which was of internal diameter 0·68 m and height 1·52 m, had its top end open. The smaller cylinder, with an external diameter of 0·50 m, had its top end closed by a 1·3 cm thick Perspex disc and, since its length was 20 cm shorter, the liquid scintillator poured into this container could fill the annular gap and the top section of the assembly.

The container was permanently installed in a light-proof wooden box which had provisions for supporting five 110 mm photomultipliers (EMI 9579 B) which were used to view this section of the screen. Four of these were placed at the bottom, equally spaced and looking upwards through short hollow light-guides into the annular cylinder of scintillator. The fifth was placed centrally on top, looking downwards into the pool of scintillator which closed the top of the Perspex cylinder. For wiring and alignment convenience, the photomultiplier bases projected through the light-tight wooden box. Inside the inner Perspex cylinder was a cylinder of 1·5 mm aluminium sheet, 0·47 m in diameter and 1·75 m long. Thus the assembly was made completely light-proof and, since the whole assembly was supported 2·2 m above the floor, the screened volume remained accessible from below without having to break the light seal. To complete the anticoincidence screening from underneath, an additional movable detector was employed which was made of a disc of NATON 11 plastic scintillator (Koch Light Laboratories), 0·44 m in diameter and 75 mm thick. It was held inside a separate light-tight container which also housed a 180 mm diameter photomultiplier (EMI type 9623 B), in optical contact with the plastic scintillator; it also served as a support for any counters or structures inserted into the screened volume. The scintillator and housing were permanently installed on a horizontal platform which could be readily raised or lowered. With the platform fully up, the plastic scintillator disc closed the base of the annular cylinder, thus completing the $4\pi$ screening, with the exception of a 30 mm annular gap

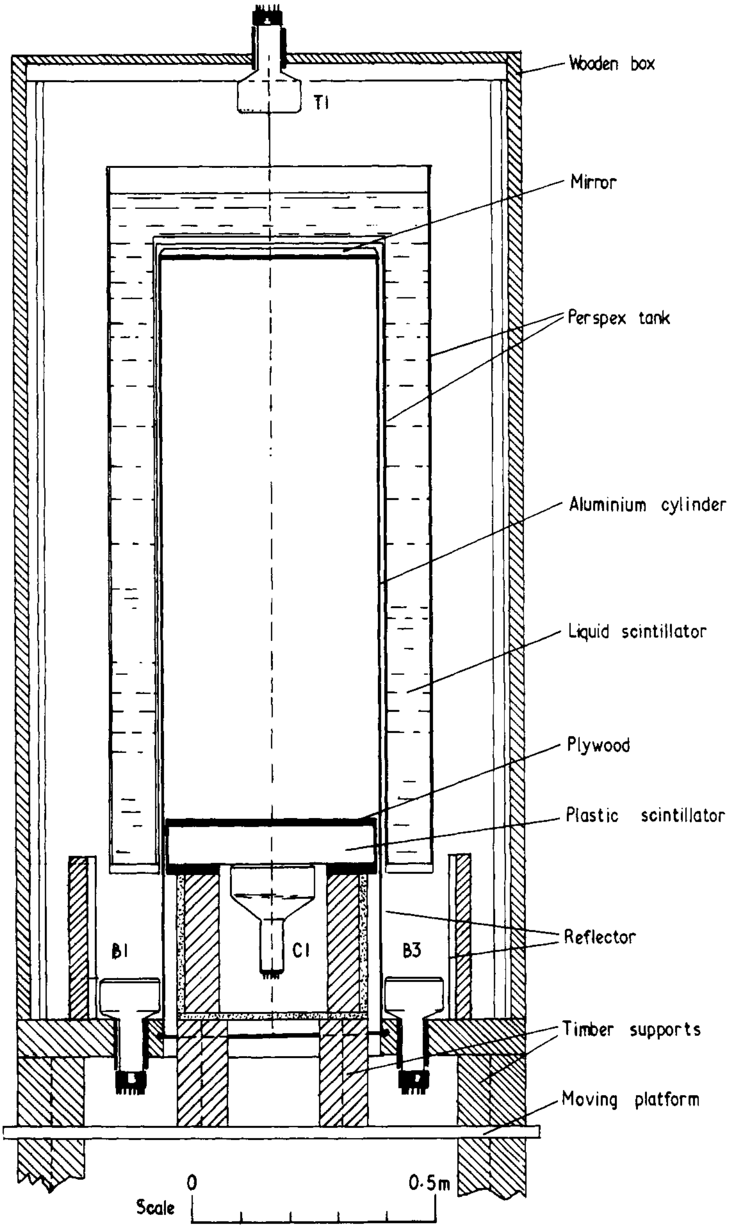


**Figure 1.** Vertical section through apparatus.

between the plastic and liquid scintillators. This provided entry for cables to any internal counters.

### *2.2. Electronics*

The outputs from each of the six screen photomultipliers were fed into individual voltage level discriminators, the outputs of which were summed by a six input 'or' gate (figure 2)

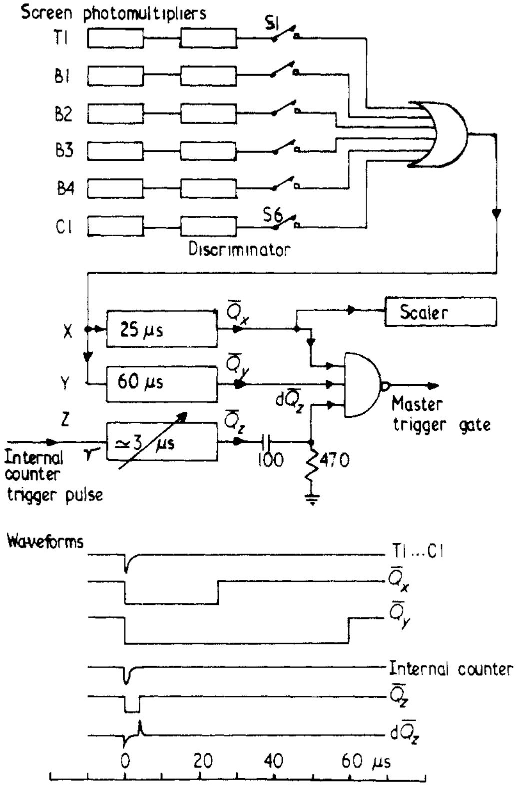


**Figure 2.** Block diagram of anticoincidence circuit.

to provide the anticoincidence signal. This triggered the two one shot multivibrators X and Y which blocked the master trigger gate, thus preventing the trigger pulses from the screened internal counter initiating the recording cycle of the equipment. An event could therefore only be recorded when it was unaccompanied by an anticoincidence pulse. The switches S1–S6 were used to connect each photomultiplier in turn through the 'or' gate to the scaler for alignment and routine checks of the counting rate during the experiment. The monostable blocking times of 25 μs and 60 μs were chosen for two purposes: (*a*) to avoid pulses due to muon decay electrons leaking through the gate, and (*b*) to avoid electronic leakage of pulses, associated with dead times inherent in such monostable circuits. With the above circuit in operation, it was calculated that (*a*) for the largest internal counter used in this experiment, pulses due to muon decay electrons leaking through were approximately 0·05 $d^{-1}$, and (*b*) approximately one in $10^8$ trigger pulses from the internal counter would arrive at times when both monostables could not be actuated by the screen photomultipliers and hence would leak into the system and be recorded as nonionizing.

It was considered important to collect as much information as possible about those interactions that did satisfy the anticoincidence criteria (ie information not only about the rates but also about the pulse heights and, in one experiment, the shape of the pulses from counters which were inserted into the screened volume). This information was obtained by employing two 128 channel logarithmic pulse height analysers of the type described by Barton *et al* (1971). Each event was then recorded as two seven bit numbers, with parity checks, on eight hole paper tape.

The recorded events were subsequently analysed by computer to form differential pulse height spectra in either one or two dimensions.

### 2.3. *Alignment, calibration and testing procedure*

The first requirement was that the effective gains of the six screen photomultipliers should be matched. This was achieved by plotting integral bias curves (counting rate as a function of supply voltage) for each photomultiplier, and adjusting the voltage to each photomultiplier until the bias curves coincided over a broad region. Since all six screen photomultipliers were fed from a single power supply (Microcell, type 411) the voltage adjustment was carried out by adjusting a shunting resistor between dynodes $D_2$ and $D_7$ and then altering a series resistor to compensate for the resulting change in potential between the remaining pairs of dynodes. After this alignment, the variation of the total counting rate for all the photomultipliers with voltage was that shown in figure 3.

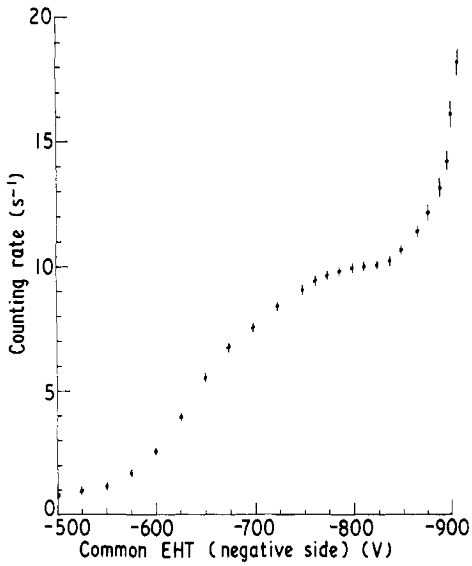


**Figure 3.** Variation of screen counting rate with photomultiplier supply voltage (after alignment).

The relatively good plateau, which has been obtained consistently over many months, shows that the optical design was satisfactory. For most of the experimental work the voltage for the photomultipliers was increased to give a total counting rate of 300 $s^{-1}$. Since figure 3 shows that the muon peak was at about 10 $s^{-1}$, this ensured that all the muons, and also some of the gamma rays scattered in the screen scintillator, were rejected. If the screen counting rate was increased very much further the anticoincidence rate was found to increase due, presumably, to the effects of circuit dead times. The optimum setting was not critical and that used caused a 'blocking' time of only 2 %.

The second requirement was that the channel width of the two pulse height analysers should be known accurately. This calibration was carried out, using a standard size pulse fed through a matched attenuator (Muirhead, type 239 A), at the beginning and the end of each individual experiment; the channel width was chosen for each experiment to meet the particular requirements of dynamic range and resolution. The long term stability of the channel width was found to be not worse than ±0·01 db per channel. The method adopted for energy calibration relied upon a knowledge of (i) the rate of energy loss of a single cosmic ray muon traversing a known thickness of scintillator material, and (ii) the track length corresponding to a particular channel number. The rate of energy loss was calculated from the formula of Sternheimer (1967) taking into account the composition of the scintillator used. The identification of a channel number with a particular track length was achieved using a Monte Carlo computer method. This program predicted the track length distribution of muons taking into account the dimensions of the counter, the assumed $\cos^2\theta$ angular distribution of the particle flux and the effect of the finite counter resolution. This method might introduce a systematic error of ±10% on all the energy scales.

In initial tests of the system, a small plastic scintillator was operated inside the screen. Once it was established that the overall behaviour was satisfactory, the apparatus was used for the five main experiments described below.

## 3. The counter telescope experiment

A counter telescope was made up of two slabs of NE 102 plastic scintillator (Nuclear Enterprises Ltd) each in the form of a rectangular parallelepiped of dimensions $28{\cdot}6 \times 20{\cdot}3 \times 5{\cdot}1\ \mathrm{cm}^3$ and viewed by a single EMI 9584 B photomultiplier tube (figure 4). Each slab of plastic scintillator was enclosed in a separate aluminium box, which housed the photomultiplier, thus forming a complete unit. Various thicknesses of lead could be

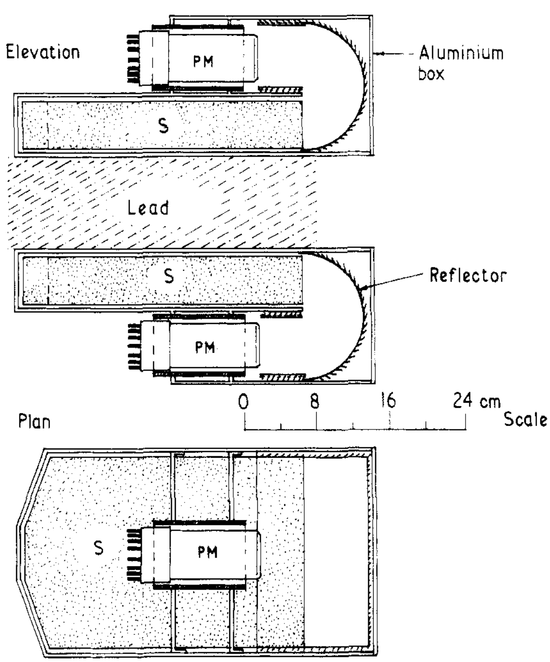


**Figure 4.** Counter telescope. S, plastic scintillator NE 102; PM, photomultiplier EMI 9584B.

placed between the counters, on top or under them, and the assembly could be placed at different positions inside the screen. The two photomultipliers were put in coincidence, with a resolving time of 0·15 μs, and the resulting signal in anticoincidence with that from the screen photomultipliers. The aperture of this telescope was 700 $cm^2$ sr.

The telescope was operated with various thicknesses of lead, and in various positions inside the screen, for a total time of 3800 h. Since the pulse heights from both counters were recorded, each experiment yielded a two dimensional distribution, and in all a very large amount of data was accumulated. A more detailed analysis is given in Pourgourides (1970), but the most important data are summarized in table 1, which reports the total rates of those events in which at least 5 MeV was recorded in each counter.

**Table 1.** Summarized results of telescope experiment

| | Position in anticoincidence screen | Thickness of lead ($g\ cm^{-2}$) | Rate ($h^{-1}$) |
|---|---|---|---|
| No anticoincidence | at bottom | 0 | 1073 ± 6 |
| No anticoincidence | at bottom | 86 | 1022 ± 5 |
| With anticoincidence | at bottom | 0 | 0·58 ± 0·05 |
| With anticoincidence | at bottom | 3·4 | 0·18 ± 0·03 |
| With anticoincidence | at bottom | 28 | 0·03 ± 0·02 |
| With anticoincidence | at bottom | 86 | 0·06 ± 0·02 |
| With anticoincidence | at bottom | 86 + additional 86 above counters | 0·01 ± 0·01 |
| With anticoincidence | at middle | 0 | 0·40 ± 0·04 |
| With anticoincidence | at top | 0 | 0·32 ± 0·04 |

These results indicate that:

(i) for penetrating ionizing particles, the screen leakage was not much worse than 1 in $10^5$ particles;

(ii) the secondaries from nonionizing particles were strongly absorbed in a few millimetres of lead;

(iii) placing the telescope at the top of the available space in the screen reduced the anticoincidence rate to about one-half the value it had when the telescope was at the bottom.

## 4. The pulse shape discrimination experiment

The nonionizing particles giving rise to the events recorded in the telescope experiment could be either photons or neutrons. The purpose of using pulse shape discrimination was to distinguish between these possibilities. A cylindrical cell, 7·6 cm by 7·6 cm, of NE 213 liquid scintillator was used as the detector, and the discrimination effected by measuring the proportion of slow component in the scintillator decay (Barton and Sanni 1965). With this arrangement it was possible to distinguish protons from electrons or muons over at least the range from 2 to 20 MeV. Again, only integral counting rates for electron energies greater than 5 MeV are given.

Calibration runs with a neutron source established that the heavily ionizing events were indeed due to protons rather than to alpha particles. Table 2 can be interpreted as showing that most of the anticoincidence events are to be attributed to photons, but that

**Table 2.** Results of pulse shape discrimination experiment

| | Time (d) | Events with apparent energy $\geqslant 5$ MeV | |
|---|---|---|---|
| | | minimum ionizing | heavily ionizing |
| No anticoincidence | 6 | 31549 | 4 |
| With anticoincidence | 13 | 809 | 7 |
| With anticoincidence and scintillator surrounded by 5 cm lead | 13 | 74 | 9 |

there is a small contribution from neutrons. The rate of the latter events was $1{\cdot}8 \pm 0{\cdot}4\, l^{-1}\, d^{-1}$ for protons of energy greater than or equal to 12 MeV (the scintillator is less efficient for heavily ionizing particles than for electrons). Using nuclear emulsions Short (1965) found a rate for knock-on protons more than twice as large per unit mass, but this difference is to be expected as many of the neutrons come from events in which other particles will trigger the anticoincidence screen.

The results of table 2 also shows that the rate of minimum ionizing events was reduced by a factor of 11 by surrounding the counter with 5 cm lead bricks. If the absorption was exponential, this would correspond to an absorption length of about $30\ g\,cm^{-2}$. In some of the preliminary experiments readings were taken with various thicknesses of lead sheet above the counter. Although the geometry of these experiments was not entirely satisfactory, they did establish that the absorption was approximately exponential and that the absorption length was almost constant over the energy range from 3 to 10 MeV.

## 5. The Cerenkov experiment

Experiments in which lead absorber had been placed above or below the two counters of the counter telescope had given some indication that the nonionizing radiation was anisotropic but the interpretation of the results was not free from ambiguity, so these experiments have not been reported. Much clearer evidence was obtained using the Cerenkov counter shown in figure 5. The radiator consisted of a cylinder of Perspex of height 21 cm and diameter 13 cm. One end face was blackened and the other viewed by a pair of 2 in photomultipliers in coincidence. (An attempt was first made using a single 5 in photomultiplier, but noise and internal Cerenkov effects in the tube made it unsatisfactory for the very low counting rates of an anticoincidence experiment.) With a nonfocusing counter of this sort, the response to particles at an angle to its axis is a complicated function which has not been investigated. For the present work it was sufficient to operate the counter as shown in figure 5 and inverted. The rates in the two positions are designated $I_d$ and $I_u$ and the anisotropy coefficient defined as

$$\eta = \frac{I_d - I_u}{I_d + I_u}.$$

The data of the experiment then give $\eta$ as a function of pulse height. The resolution of this counter was much worse than that of the scintillation counters which increased the

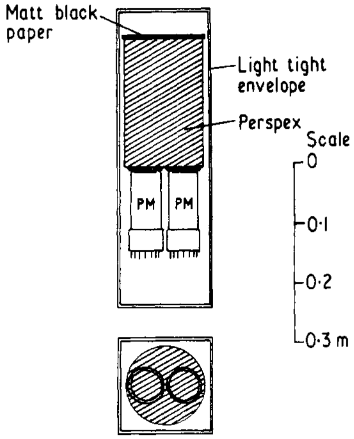


**Figure 5.** Cerenkov counter.

uncertainty in converting pulse heights to energies. With this caution, the variation of anisotropy with energy is presented in figure 6.

With the anticoincidence switched off, the higher energy events would be mainly due to muons which are known to have a $\cos^2\theta$ distribution at this depth underground. The value of $\eta$ should therefore be unity, and the observation of this value experimentally can be regarded as a check on the operation of the counter. At lower energies the presence of scattered secondary particles explains the reduction in the value of $\eta$; it should become zero in the radioactive region. For the anticoincidence events $\eta$ was always less than unity, indicating that the radiation responsible must have had a broad angular distribution, but it is important to note that it was not isotropic; the significance of this distribution will be discussed in § 7.

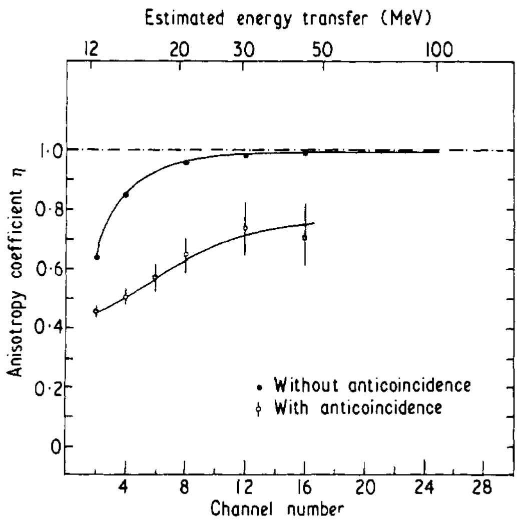


**Figure 6.** Variation of anisotropy with energy.

## 6. The large volume counter experiments

This experiment was designed to take advantage of the large space screened by the anticoincidence counter. It consisted of a cylindrical Perspex container of internal diameter 40·5 cm and height 1 m, which could be filled to any depth with medicinal paraffin based liquid scintillator. This was viewed by a pair of 5 in photomultipliers (type 9618 R) from a distance of 18 cm above the surface of the scintillator. As in the previous experiment, it was found essential to operate the two photomultipliers in coincidence to avoid spurious effects. Two series of experiments were carried out with this counter.

### *6.1. Pulse height spectra*

Results were obtained for five different depths of liquid and are summarized in table 3.

**Table 3.** Anticoincidence rates in large counter

| Scintillator depth (cm) | Scintillator volume (l) | Time (d) | Integral anticoincidence rate per unit volume ($l^{-1}$ $d^{-1}$) | | |
|---|---|---|---|---|---|
| | | | $E > 10$ MeV | $E > 20$ MeV | $E > 40$ MeV |
| 7·6 | 9·5 | 10·4 | 15·5 ± 0·4 | 2·5 ± 0·2 | 0·25 ± 0·05 |
| 15·2 | 19·0 | 11·4 | 20·2 ± 0·4 | 4·0 ± 0·2 | 0·44 ± 0·05 |
| 30·5 | 38 | 10·2 | 21·0 ± 0·4 | 4·6 ± 0·2 | 0·62 ± 0·05 |
| 40·6 | 51 | 2·7 | 19·4 ± 0·4 | 4·4 ± 0·2 | 0·75 ± 0·08 |
| 62·5 | 78 | 5·7 | 13·7 ± 0·4 | 3·2 ± 0·2 | 0·43 ± 0·09 |

It is seen that the anticoincidence rates were approximately proportional to the volume of the detector, with some reduction at both small and large depths. This is reasonable if the events were due to photons as at small thicknesses some of the secondary electrons would have had sufficient energy to reach the anticoincidence screen, whilst at depths much greater than the attenuation length of photons the number of available photons would have been reduced. Any detailed quantitative analysis is of doubtful value because of the variation of anticoincidence rate with position, as reported in § 3, and because the angular distribution is not known, but the general behaviour is at least reasonable.

Figure 7 shows the pulse height distributions for the largest volume of scintillator. It will be noted that with this geometry there is no clear muon peak; Monte Carlo studies have shown that the shape of the upper curve is that to be expected for a counter of height one and a half times its diameter and a $\cos^2\theta$ angular distribution of muons. The proportion of anticoincidence events is greater than found in the telescope experiment because there was no space to surround this large counter with lead.

### *6.2. Muon decays*

The purpose of this experiment was to investigate the production of muons by neutral components of the cosmic radiation underground. The circuit was modified so that events were only recorded if a pair of pulses arrived within an interval of 12 μs: the time

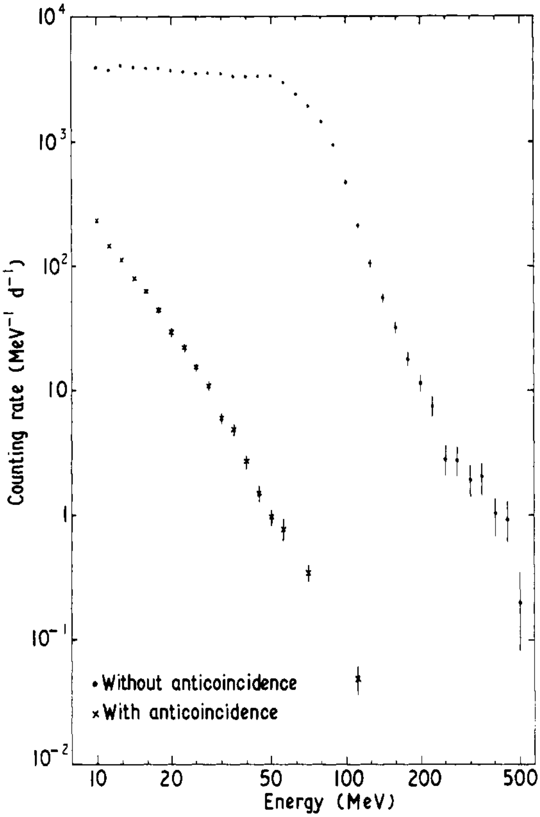


**Figure 7.** Pulse height spectra for large counter (78 l).

between the two pulses was measured using a 10 MHz clock. In the anticoincidence runs it was required that there was no pulse from the screen at the time of occurrence of the first pulse, but no account was taken of whether the screen gave an output at the time of the second pulse. The purpose of the latter arrangement was to permit a decay electron to escape from the inner counter without causing the event to be cancelled.

The time distributions for 3915 pairs of pulses in a run of 3·8 d without the anticoincidence and for 8 pairs in 46 d with it operating are shown in figure 8. In the first case the distribution is exponential, with a fitted decay constant of $2{\cdot}230 \pm 0{\cdot}035$ μs, which shows that the apparatus was functioning correctly. After correcting for events lost because one or both pulses were below the accepted levels, because the decay time was outside the accepted range or because some negative muons would have been captured before decaying, the rate for stopping muons was found to be $23 \pm 2 \times 10^{-3}$ g$^{-1}$ d$^{-1}$. This agrees with two other measurements in the same laboratory: Short (1963) found $19 \pm 1{\cdot}5 \times 10^{-3}$ g$^{-1}$ d$^{-1}$ in emulsion, corresponding to $27 \pm 2 \times 10^{-3}$ g$^{-1}$ d$^{-1}$ in scintillator, and Barton and Slade (1965) found $26 \pm 3 \times 10^{-3}$ g$^{-1}$ d$^{-1}$.

The time distribution of the anticoincidence events is clearly not the same. Most of them are certainly to be interpreted as the accidental traversal of a muon within the 12 μs period after a normal anticoincidence event. The rate of these accidentals is readily calculated and leads to a prediction of 7 events in 46 d. The same hypothesis would predict that these events should be uniformly distributed in time, as are the observed ones.

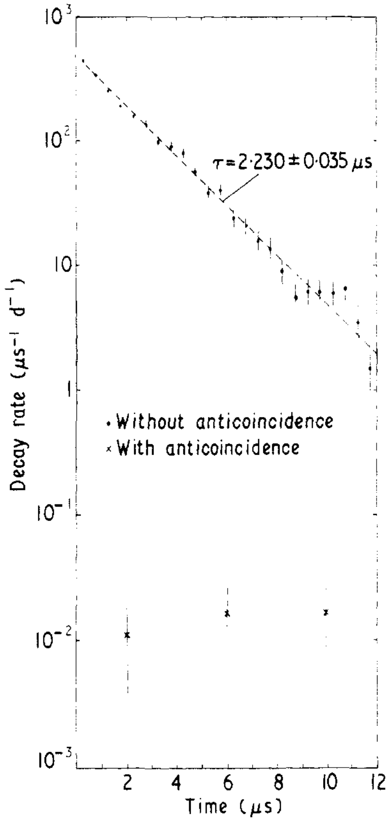


**Figure 8.** Decay time distributions for large counter (78 l).

From these data it is possible to deduce an upper limit for the rate at which any neutral radiation produces muons. The result can most conveniently be expressed as the product of flux times interaction cross section. Since any such neutral radiation is likely to be penetrating, it is assumed to be isotropic; for a collimated radiation the numerical values would be increased. The result, together with previous estimates, is shown in table 4.

The present experiment is in direct contradiction with that of Cowan *et al* (1969) unless the cross section is large enough for the radiation to be strongly absorbed.

**Table 4.** Estimates of production rate of muons by neutral radiation

| Reference | Location | $\Phi\sigma$ ($sr^{-1}\ s^{-1}$ nucleon$^{-1}$) |
|---|---|---|
| Cowan *et al* (1969) | sea level | 'about' $3\times10^{-33}$ |
| Ashton *et al* (1969) | sea level | $<4\times10^{-33}$ |
| This experiment | 60 hg cm$^{-2}$ | $<3\times10^{-36}$ |
| Bergamasco *et al* (1970) | 4500 hg cm$^{-2}$ | $<3\times10^{-38}$ |

(For the present experiment the confidence level for the limit is 95%; the other authors do not give confidence levels.)

## 7. Analysis

The results of the various experiments can be summarized as follows:

(i) most of the anticoincidence events give rise to lightly ionizing secondaries, but there is a small contribution from neutrons.

(ii) The absorption length of the nonionizing radiation is compatible with that of photons.

(iii) The nonionizing radiation is mostly directed downward with an angular distribution broader than that of muons at the same depth.

(iv) The rate of events is smaller when the detector is near the top of the screened volume.

(v) There is no evidence for anomalous particles.

None of the evidence contradicts the hypothesis that the radiation is mainly composed of photons. The problem then is to explain the origin of these photons in such a way that it accounts for the absolute number, the energy spectrum, the angular distribution and the variation with position of the events produced by them. The data from the various experiments depend only slightly on the volume of scintillator used, as can be seen in figure 9. Some of the events of only a few MeV could be due to radioactive

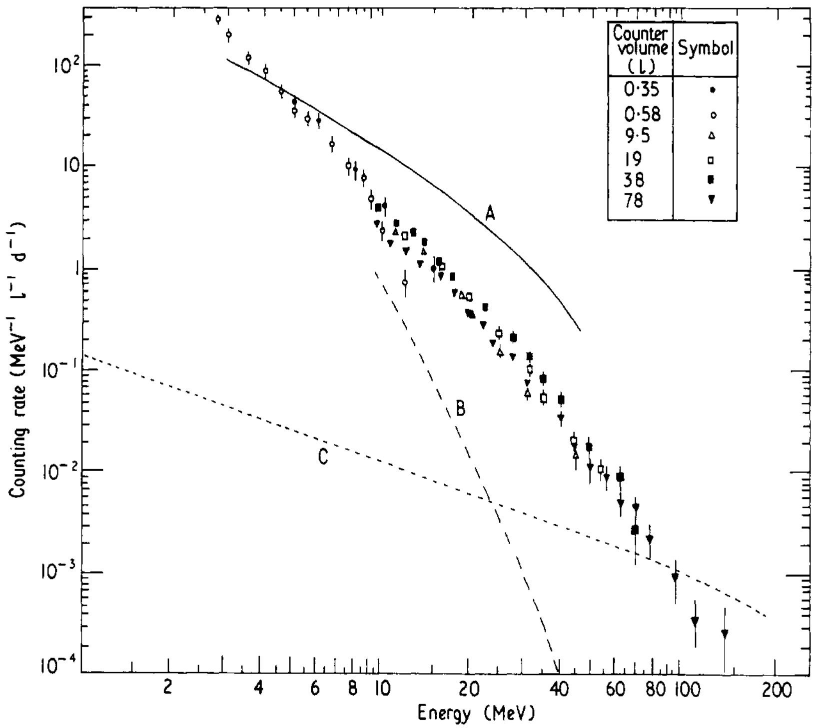


**Figure 9.** Anticoincidence rate per unit volume in large counter. A, knock-on bremsstrahlung; B, muon decay bremsstrahlung; C, muon bremsstrahlung.

processes but at higher energies they must be produced, directly or indirectly, by the muon beam. Possible processes are:

(i) muon bremsstrahlung;

(ii) bremsstrahlung from muon decay electrons;
(iii) contribution from muon nuclear events;
(iv) bremsstrahlung from electrons knocked on by muons;
(v) bremsstrahlung from pair produced electrons;
these will be considered in turn.

### 7.1. *Muon bremsstrahlung*

Using the known muon spectrum and the radiation probability given by Petrukhin and Shestakov (1967) the resulting photon spectrum has been computed and the resulting interaction rate plotted on figure 9. However, the photon is usually emitted at such a small angle that the muon will strike the anticoincidence screen and the event will not be accepted. Hence this process cannot explain more than a small fraction of the events, even at the highest energy considered here.

### 7.2. *Bremsstrahlung from muon decay electrons*

The results in §§ 6.1 and 6.2 show that the rate for anticoincidence events with $E > 10$ MeV is about the same as the stopping rate for muons. The mean energy of the electrons from muon decay is about 40 MeV; this is less than the critical energy in rock, and a rough calculation shows that the probability of the decay electron radiating a photon of more than 10 MeV before it comes to rest is about one quarter. Thus the interaction rate of photons due to this mechanism is at most one quarter of that observed. In fact only a proportion of these events will be observed as in some cases either the incident muon or the decay electron will penetrate the anticoincidence screen.

There are two other reasons why this process cannot explain the observed events. Firstly, it would predict a sharp cut-off at the maximum decay energy of 53 MeV. Secondly, it would predict an approximately isotropic angular distribution (the effects due to muon polarization are negligible). Neither prediction is supported by the data, and it is clear that this process is not the major source of the observed events. However, the arguments given above show that it does contribute a proportion of the events at lower energies; the broken curve shown on figure 9 is an estimate of this effect.

### 7.3. *Contribution from muon nuclear events*

It is well established that the energy lost by muons in nuclear collisions is only a fraction of that lost in bremsstrahlung. Since not more than one-third of the energy in a nuclear cascade can appear as photons, the total contribution is at least an order of magnitude smaller than that considered in § 7.1 and is therefore insignificant.

### 7.4. *Bremsstrahlung from electrons knocked on by muons*

The process considered here is that shown in figure 10. It might at first seem that the contribution to the observed anticoincidences would be small as the energy spectrum of knock-on electrons, the probability of bremsstrahlung and the mean angle of bremsstrahlung are all relatively unfavourable. On the other hand the mean angle of multiple scattering, before the photon is emitted, will be shown below to be quite large and this makes the process of considerable significance. An exact theory would be extremely involved as it would have to take account of the complicated geometry of the apparatus.

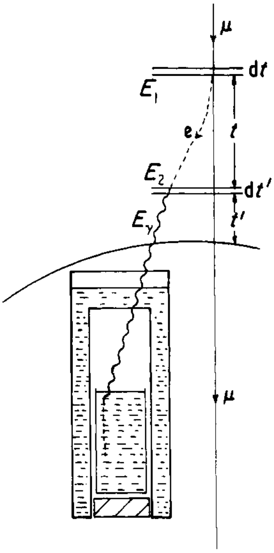


**Figure 10.** Diagram of photon production by muon knock-on.

Instead an approximate theory is developed in which the total number and energy spectrum of the photons is first calculated and then their mean angle of deviation.

The notation and geometry is that given in figure 10. The assumptions made are: (i) integrated intensity of muons at this depth $J_1 = 70\ \mathrm{cm}^{-2}\,\mathrm{d}^{-1}$; (ii) knock-on probability in d$t$ is

$$N(E_1) = \frac{A\,\mathrm{d}t}{E_1^2} \qquad (\mathrm{MeV}^{-1}\,\mathrm{g}^{-1}\,\mathrm{cm}^2\,\mathrm{muon}^{-1})$$

where $A = 0{\cdot}07$ MeV; (iii) rate of energy loss $-\mathrm{d}E/\mathrm{d}x = a = 1{\cdot}8\ \mathrm{MeV\,g^{-1}\,cm^{-2}}$ (ie $E_2 = E_1 - at$); (iv) the radiation probability is

$$P(E_2, E_\gamma) = \frac{C}{E_\gamma}\left\{1 - \frac{E_\gamma}{E_2}\left(1 - 0{\cdot}2\ln\frac{E_2}{10}\right)\right\} \qquad (\mathrm{MeV}^{-1}\,\mathrm{g}^{-1}\,\mathrm{cm}^2)$$

with $C = 4{\cdot}5 \times 10^{-2}$. (This is an approximate fit to the expression given in Rossi (1952) and is valid for $E_2 < 50$ MeV.)

The photons are absorbed in the rock with an absorption coefficient $\mu \simeq 0{\cdot}03\ \mathrm{g}^{-1}\,\mathrm{cm}^2$ for $E_\gamma < 50$ MeV. At energies greater than this, which is approximately the critical energy for rock, much more detailed argument is necessary but will not be considered here. By cutting off the integral at 50 MeV only, a lower limit to the photon flux is estimated.

With the above assumptions the photon flux emerging from the tunnel roof is

$$N(E_\gamma) = \int_{t=0}^{\infty}\int_{t'=0}^{\infty}\int_{E_2=E_\gamma}^{50} J_1 \frac{A\,\mathrm{d}t}{(E_2 + at)^2}\,\mathrm{e}^{-\mu t'}\,\mathrm{d}t' P(E_2, E_\gamma)\,\mathrm{d}E_2$$

where the contribution from outside the given energy limits is neglected.

Multiplying by $\mu$ gives the interaction rate, and this is plotted on figure 9; it is seen that this effect is a much more significant one than those considered in previous sections. However, we must next investigate what proportion of these photon interactions would be rejected because the muon triggers the screen. As a first step towards determining this proportion, it is convenient to calculate the mean angle at which photons of a given energy deviate from the muons producing them. This angle is mainly the result of the multiple scattering which the knock-on electron undergoes before the photon is radiated.

For an electron in rock the projected angle of scattering in thickness $\delta t$ is given by

$$\overline{\delta\theta^2} = \frac{\alpha}{E^2}\,\delta t$$

with $\alpha = 8{\cdot}0\ \mathrm{rad^2\,MeV^2\,g^{-1}\,cm^2}$ for 'standard' rock. So the mean square deviation of the electron is

$$\overline{\theta^2} = \int_0^t \frac{\alpha}{(E_1 - ax)^2}\,\mathrm{d}x = \frac{\alpha}{a}\left(\frac{1}{E_2} - \frac{1}{E_2 + at}\right).$$

The average of this quantity for all electrons giving rise to photons of energy $E_\gamma$ will give the mean square deviation of the latter

$$\overline{\theta^2_{E_\gamma}} = \left\{\int_{t=0}^{\infty}\int_{E_2=E_\gamma}^{50} \frac{J_1 A\,\mathrm{d}t}{(E_2+at)^2} P(E_2, E_\gamma)\frac{\alpha}{a}\left(\frac{1}{E_2} - \frac{1}{E_2+at}\right)\mathrm{d}E_2\right\}$$
$$\times\left\{\int_{t=0}^{\infty}\int_{E_2=E_\gamma}^{50} \frac{J_1 A\,\mathrm{d}t}{(E_2+at)^2} P(E_2, E_\gamma)\,\mathrm{d}E_2\right\}^{-1}.$$

This expression is only a first approximation, but its importance is that it predicts quite large angles. For example, for $E_\gamma = 10$ MeV, the root mean square angle is almost 0·3 rad. No allowance has been made for the angular deviation of the radiated photon from the electron, but this angle is only about one-tenth as large and can be neglected. Referring to figure 10, which has been drawn to scale and for an angle of 0·3 rad, it is clear that in a high proportion of events the muon creating a photon will not strike the anticoincidence screen. At higher energies this will still be true: to the same approximation the angle of 30 MeV photons is 0·18 rad. The probability of the photon being well separated from the muon will of course increase with distance from the tunnel roof so that the variation of anticoincidence rate with position in the screen, noted in § 3, is readily understood. Also it is understandable that the observed angular distribution is broader than for muons but not isotropic.

This very rough analysis seems sufficient to show that knock-on electrons provide a source of photons sufficient to explain the observed events. The difference between the slope of the experimental and theoretical curves is not surprising, as at higher energies more of the electrons produced in the counter will have long enough tracks to reach the anticoincidence screen and cause the event to be cancelled.

### *7.5. Bremsstrahlung from pair produced electrons*

Some photons must be produced by this mechanism, but the total energy lost by muons in pair production is only comparable to that lost by direct bremsstrahlung. Since the latter process was shown above to be unimportant, it follows that a less direct means of producing photons must be even less so.

## 8. Conclusions

The above analysis shows that the only important sources of photons are bremsstrahlung from electrons produced either by muon decay or by muon knock-on. The former source would be an almost isotropic one and cannot explain more than at most a quarter of the events. Semiquantitative arguments have established that bremsstrahlung from electrons knocked on by muons is sufficient to account for the observed effects. The involved geometry of the experiment makes it very difficult to develop an exact theory, and it does not appear that much could be learnt from such an attempt.

The only experiment with which it is useful to compare the present one is that described by Giamati and Reines (1962). They used 200 l of scintillator, screened by 23 cm of steel and an anticoincidence Cerenkov counter, at a depth of 1440 hg $cm^{-2}$ underground. In this experiment their anticoincidence performance was relatively poor, but later Kropp and Reines (1965), after making various technical improvements in the apparatus, observed only 21 events of more than 10 MeV in 187 d. Thus their rate was less than that reported in table 3 by a factor of $2{\cdot}5 \times 10^4$. The ratio of muon intensities at the two depths is $1{\cdot}5 \times 10^3 : 1$ and the remaining difference may well be attributed to the use of thick steel screening. It seems quite possible that Kropp and Reines have underestimated the contribution from muon produced photons, and consequently their lower limit for proton lifetime ($\simeq 10^{28}$ years) could be revised upwards.

The main conclusion from this experiment is that the nonionizing radiation underground does not display any anomalous features. It should therefore be possible to design counters for particular low background counting experiments such as solar neutrino detection. At greater depths underground the background will be reduced in proportion to the muon intensity, although at sufficiently great depth the contribution from nuclear events will become relatively more important. A larger apparatus of similar geometry to the present one need not lead to an intolerably large increase in the 'blocking' time, because the anticoincidence screen design is efficient. A specific recommendation can be made that any apparatus should be placed as close to the tunnel roof as possible since this will minimize the lateral separation of muons from secondary neutrons or photons.

## Acknowledgments

The apparatus was constructed by the technical staff of the department under the direction of Mr G W Dickson. We are indebted to Dr I W Rogers for useful discussions and help with the computer analysis, and to Mr J P Betts for taking some of the data.

## References

Ashton F, Edwards H J and Kelly G N 1969 *Proc. 11th Int. Conf. on Cosmic Rays Budapest* (1969 *Acta Phys. Hung. Suppl.* **29** 347–51)

Barton J C, Barnaby C F, Jasani B M and Thompson C W 1962 *J. sci. Instrum.* **39** 360–3

Barton J C, Munas A F and Wright A G 1971, *Nucl. Instrum. Meth.* **92** 89–91

Barton J C and Sanni A O 1965 *Proc. 9th Int. Conf. on Cosmic Rays, London* (London: The Institute of Physics and The Physical Society) pp 1094–6

Barton J C and Slade M 1965 *Proc. 9th Int. Conf. on Cosmic Rays, London* (London: The Institute of Physics and The Physical Society) pp 1006–8

Bergamasco L, Castagnoli C and Maringelli M 1970 *Lett. Nuovo Cim.* **3** 159–62
Cowan C, Ryan D and Buckwalter G 1965 *Proc. 9th Int. Conf. on Cosmic Rays, London* (London: The Institute of Physics and The Physical Society) pp 1041–4
Cowan C L *et al* 1969 *Proc. 11th Int. Conf. on Cosmic Rays, Budapest* (1969 *Acta Phys. Hung. Suppl.* **29** 107–19)
Giamati C C and Reines F 1962 *Phys. Rev.* **126** 2178–87
Kropp W R and Reines F 1965, *Phys. Rev.* **137** B740–51
Moe M K, Jenkins T L and Reines F 1964 *Rev. sci. Instrum.* **35** 370–2
Petrukhin A A and Shestakov V V 1967 *Can. J. Phys.* **46** S377–80
Pourgourides C M 1970 *PhD Thesis* University of London
Rossi B 1952 *High Energy Particles* (New York: Prentice-Hall)
Short A M 1963 *Proc. Phys. Soc.* **81** 841–5
—— 1965 *Proc. 9th Int. Conf. on Cosmic Rays, London* (London: The Institute of Physics and The Physical Society) pp 1009–11
Stenberg A and Olsson I U 1968 *Nucl. Instrum. Meth.* **61** 125–33
Sternheimer R M 1967 *Phys. Rev.* **164** 349–51
Wogman N A, Perkins R W and Kaye J H 1969 *Nucl. Instrum. Meth.* **74** 197–212